

Characterization, Separation Performance, and Model Analysis of STPP-Chitosan/PAN Polyelectrolyte Complex Membranes

Xiao-Hua Ma,^{1,2} Zhen-Liang Xu,^{1,2} Chao-Qing Ji,² Yong-Ming Wei,² Hu Yang²

¹State Key Laboratory of Chemical Engineering, East China University of Science and Technology (ECUST), Shanghai 200237, China

²Membrane Science and Engineering R&D Lab, Chemical Engineering Research Center, ECUST, Shanghai 200237, China

Received 25 March 2010; accepted 17 August 2010

DOI 10.1002/app.33216

Published online 8 November 2010 in Wiley Online Library (wileyonlinelibrary.com).

ABSTRACT: Polyelectrolyte complex membranes (PCMs) were prepared using sodium tripolyphosphate (STPP) solution surface-crosslinking chitosan/polyacrylonitrile (PAN) composite membranes. Fourier transform infrared (FTIR) was used to characterize the surface-crosslinking. The effects of different surface-crosslinking time on morphologies, element distribution, and crystal structures were investigated by scanning electron microscopy (SEM), energy dispersion of X-ray (EDX), and X-ray diffraction (XRD). The effect of crosslinking ratio on swelling ratio was analyzed. The separation performances of PCMs in terms of permeation flux and separation factor were measured by dehydrating ethyl acetate aqueous solutions. A kinetic model of crosslinking reaction was proposed to investigate the effect of crosslinking agent concentration and surface-crosslinking time on the crosslinking ratio of

PCMs. It was found that the membrane possessed the excellent performance when surface crosslinked for 15 min. The permeation flux and separation factor were 336 g/(m² h) and 6270 in 97 wt % ethyl acetate aqueous solution at 313 K. The crosslinking ratio of PCM exponentially increased as time increased, while linearly increased as concentration and diffusion coefficient of crosslinking agent STPP solution increased. And the effect of crosslinking agent concentration on crosslinking ratio was inversely proportional to surface-crosslinking time. The experimental results matched well with the kinetic model when STPP concentration was lower than 5 wt %. © 2010 Wiley Periodicals, Inc. *J Appl Polym Sci* 120: 1017–1026, 2011

Key words: polyelectrolytes; membranes; kinetics; crosslinking; separation techniques

INTRODUCTION

Pervaporation is recognized as an effective process to separate azeotropic mixtures, close-boiling mixtures, isomers, and mixtures consisting of heat-sensitive compounds, and it has been widely used in dehydration of water/organic mixtures, removal of organic from aqueous solutions, and separation of organic/organic mixtures.¹ Polyelectrolyte complex membrane (PCM) is one of the most promising pervaporation membranes, which is effective for the dehydration of organics due to inherently ionic crosslinked and highly hydrophilic.^{2–5}

Chitosan has been applied in medicine and pharmacy, in paper and textile industry, in environmen-

tal remediation, and other industrial areas due to its excellent properties such as biocompatibility, biodegradability, nontoxicity, adsorption properties, and so on.⁶ However, the poor solubility of chitosan limits its application and makes itself inconvenient in processing. Versatile modifications are performed on the hydroxyl and amino groups of glucosamine units of chitosan, and physicochemical properties of the modified chitosan are possibly tailored.⁷ Crosslinking on chitosan is a convenient and effective way to improve its physical and mechanical properties for practical applications, since crosslinking can avoid the dissolution of hydrophilic polymer chains or segments into aqueous. Once crosslinking reaction between different polymer chains is introduced, the obtained networks show visco-elastic and sometimes pure elastic behavior.⁷

Several studies have been carried out to utilize polyelectrolyte complexes in pervaporation.⁸ However, the application of solid polyelectrolyte complexes is greatly limited in membrane separation fields because of the difficulty in preparing homogeneous PCM through traditional solvent method or thermal method.⁹ Richau et al.^{10,11} reported that

Correspondence to: Z.-L. Xu (chemxuzl@ecust.edu.cn).

Contract grant sponsor: Key Technology R&D Program of China; contract grant number: 2009ZX02032.

Contract grant sponsor: Chemistry and Chemical Technology Research Center Plan of Shanghai Huayi Group; contract grant numbers: A200-8608, A200-80726.

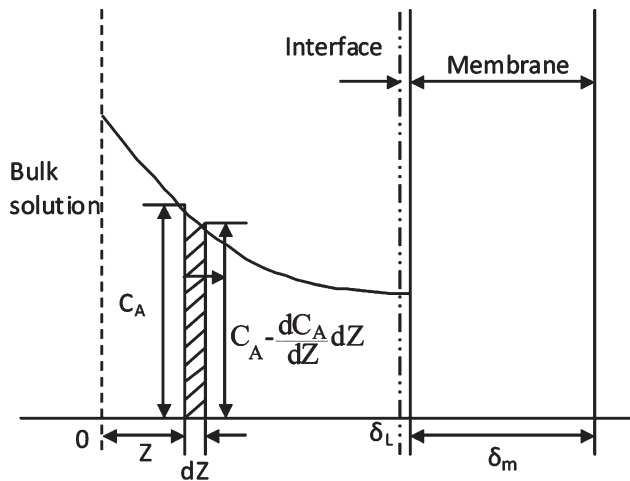


Figure 1 Schematic of mass transfer and concentration distribution in surface-crosslinking reaction process.

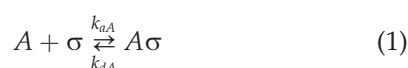
introducing surface reaction method could solve this problem. One polyelectrolyte solution is coated onto a glass plate or micro-porous substrate, whose surface is then coated or spin-coated by the other polyelectrolyte solution. The membrane obtained by this means, which is macroscopically inhomogeneous along its cross section, was found to have good selectivity due to its lower swelling degree through ionic crosslinking structure.¹² Although this surface reaction method has artfully avoided treating solid polyelectrolyte complexes, the ionic crosslinking degree of polyelectrolyte complexes formed on the interface of PCM has not been controlled and in most cases both polyelectrolytes are fully neutralized.

This article investigates the effect of crosslinking ratio on the structure and performance of PCM. A kinetic model has been proposed to analyze the effect of crosslinking agent concentration and surface-crosslinking time on crosslinking ratio of PCMs, which is used to fit with experimental data.

THEORY

Figure 1 shows the mass transfer and concentration distribution of surface-crosslinking process. Crosslinking agent A diffuses from the bulk solution to the surface of membrane due to the driving force of concentration gradient. A is adsorbed on the surface of the membrane. The surface-crosslinking reaction occurs when A is adsorbed on the active centers of membrane. Assuming the mechanism of the surface-crosslinking reaction $A \rightarrow R$ can be given as follows:

Adsorption process of A :



Surface-crosslinking reaction process:



where σ represents active center on the surface of membrane; R is the polyelectrolyte complex; k_{aA} is the adsorption rate constant; k_{dA} is the desorption rate constant (mol/m^2); and k is the surface-crosslinking reaction rate constant (mol/m^2).

According to mass balance, between the bulk solution and the surface of membrane,

$$-D_A \frac{\partial^2 C_A}{\partial Z^2} = \frac{dC_A}{dt} \quad (3)$$

where D_A is the diffusion coefficient of A ; C_A is the concentration of A (mol/m^2); Z is the distance from the bulk solution to the surface of membrane (m); and t is the accumulation time (h).

On the surface of membrane,

$$\frac{dC_{A\sigma}}{dt} = k_{aA} C_A(\delta_L) C_\sigma(0) (1 - \theta_A - \theta_R) - k_{dA} C_\sigma(0) \theta_A - k C_{A\sigma} \quad (4)$$

where $\theta_R = \frac{C_R}{C_\sigma(0)}$ is the crosslinking ratio of A on the surface of membrane; $\theta_A = \frac{C_{A\sigma}}{C_\sigma(0)}$ is the adsorption ratio of A on the surface of membrane; and $C_\sigma(0)$ is the saturation adsorption concentration on the surface of membrane (mol/m^2).

It is assumed that the crosslinking reaction rate is much slower than the adsorption rate on the surface of membrane. Langmuir equation is used to describe the adsorption equilibrium.

$$\theta_A = \frac{K_A C_A(\delta_L)}{1 + K_A C_A(\delta_L)} (1 - \theta_R) \quad (5)$$

where K_A is the adsorption equilibrium constant (m^2/mol), $K_A = \frac{k_{aA}}{k_{dA}}$.

The boundary conditions for eq. (3) are

$$t = 0; \quad Z = 0, C_A = C_A(0); \quad Z = \delta_L, C_A = C_A(\delta_L) \quad (6)$$

where $t = 0$ refers to the time when adsorption reaches equilibrium. Equation (4) can be reduced to

$$\frac{dC_{A\sigma}}{dt} = -k C_{A\sigma} \quad (7)$$

Based on eqs. (1) and (2),

$$-\frac{dC_A}{dt} = \frac{dC_{A\sigma}}{dt} = -\frac{dC_R}{dt} \quad (8)$$

The following equation is obtained

$$\frac{d\theta_R}{dt} = k \frac{K_A C_A(\delta_L)}{1 + K_A C_A(\delta_L)} (1 - \theta_R) \quad (9)$$

Solution eq. (9), the crosslink ratio of PCM can be expressed as

$$\theta_R = 1 - \exp\left(-\frac{K_A C_A(\delta_L)}{1 + K_A C_A(\delta_L)} t\right) \quad (10)$$

Solution eq. (3) results in

$$C_A(z, t) = \left(A_1 \exp\left(\sqrt{\frac{\beta}{D_A}} z\right) + B_1 \exp\left(-\sqrt{\frac{\beta}{D_A}} z\right) \right) C_1(t) \exp(-\beta t) \quad (11)$$

When the adsorption of A on the surface of membrane reaches equilibrium, $\frac{dC_A(\delta_L)}{dz} = 0$. Based on eqs. (6) and (11),

$$A_1 = \frac{C_A(\delta_L)}{2} \exp\left(-\sqrt{\frac{\beta}{D_A}} \delta_L\right) \quad (12)$$

$$B_1 = \frac{C_A(\delta_L)}{2} \exp\left(\sqrt{\frac{\beta}{D_A}} \delta_L\right)$$

According to eqs. (8) and (10),

$$\beta = k \frac{K_A C_A(\delta_L)}{1 + K_A C_A(\delta_L)} \quad (13)$$

$$C_1(t) = C_\sigma(0) (\text{coefficient})$$

Equation (11) can be written as

$$C_A(z, t) = C_A(\delta_L) \text{ch}\left(\sqrt{\frac{kK_A C_A(\delta_L)}{D_A(1 + K_A C_A(\delta_L))}} (z - \delta_L)\right) C_\sigma(0) \exp\left(-\frac{kK_A C_A(\delta_L)}{D_A(1 + K_A C_A(\delta_L))} t\right) \quad (14)$$

In eq. (14),

$$\text{ch}\left(\sqrt{\frac{kK_A C_A(\delta_L)}{D_A(1 + K_A C_A(\delta_L))}} (z - \delta_L)\right) = \frac{\exp\left(\sqrt{\frac{kK_A C_A(\delta_L)}{D_A(1 + K_A C_A(\delta_L))}} (z - \delta_L)\right) + \exp\left(-\sqrt{\frac{kK_A C_A(\delta_L)}{D_A(1 + K_A C_A(\delta_L))}} (z - \delta_L)\right)}{2}$$

Based on eq. (8), the crosslinking ratio of PCM can be expressed as

$$\theta_R = \frac{1}{C_\sigma(0)} \int_0^t \int_0^{\delta_L} C_A(Z, t) dt dZ \quad (15)$$

Substituting eq. (14) into eq. (15) results in

$$\theta_R = M[1 - \exp(-Nt)] \quad (16)$$

In eq. (16),

$$M = C_A(0) \left(\frac{kK_A C_A(\delta_L)}{1 + K_A C_A(\delta_L)}\right)^{-\frac{3}{2}}$$

$$\times \sqrt{D_A} th\left(\sqrt{\frac{kK_A C_A(\delta_L)}{D_A(1 + K_A C_A(\delta_L))}} \delta_L\right)$$

$$N = \frac{kK_A C_A(\delta_L)}{1 + K_A C_A(\delta_L)}$$

$$th\left(\sqrt{\frac{kK_A C_A(\delta_L)}{D_A(1 + K_A C_A(\delta_L))}} \delta_L\right) = \frac{\exp\left(\sqrt{\frac{kK_A C_A(\delta)}{D_A(1 + K_A C_A(\delta))}} \delta_L\right) - \exp\left(-\sqrt{\frac{kK_A C_A(\delta)}{D_A(1 + K_A C_A(\delta))}} \delta_L\right)}{\exp\left(\sqrt{\frac{kK_A C_A(\delta)}{D_A(1 + K_A C_A(\delta))}} \delta_L\right) + \exp\left(-\sqrt{\frac{kK_A C_A(\delta)}{D_A(1 + K_A C_A(\delta))}} \delta_L\right)}$$

It is obvious that the crosslinking ratio of PCM exponentially increases as time increases, and line-

arly increases as concentration and diffusion coefficient of crosslinking agent solution increase.

EXPERIMENTAL

Materials

Chitosan (80% N-deacetylation degree, the average molecular weight M_w is 2.5×10^5 g/mol) was obtained from Shanghai Wei-Kang Biological Products (China). STPP ($\text{Na}_5\text{P}_3\text{O}_{10}$) was purchased from Zhejiang Fu-Zhou Food Chemical (China). All other solvents and reagents were obtained from Shanghai Chemical Reagent (China). All the water used in this work was deionized water.

Polyacrylonitrile (PAN) ultrafiltration (UF) flat support membranes were prepared in the lab (pure water flux: 13.6 L/(m² h·Bar), BSA rejection: 95% (0.1 MPa)).

Gas chromatograph (Techcomp, GC7890 China) equipped with a thermal conductivity detector (TCD) and a GDX-102 packed column was used to measure the composition of feed liquid and permeate liquid.

Membrane preparation

Chitosan was dissolved in an aqueous solution of 2 wt % acetate acid at 25°C and stirred at a low speed for 24 h to prepare 2.5 wt % coating solution. After removing the insoluble impurities, the coating solution was

defoamed to remove air bubbles. Then the above solution was coated onto PAN UF support membrane, which was described in detail elsewhere,¹³ and dried at 25°C. The dried chitosan/PAN composite membranes were immersed into STPP solution with different concentrations (1, 5, 10, and 15 wt %, which were labeled as PCM-1, PCM-2, PCM-3, and PCM-4, respectively) to surface crosslink. The surface-crosslinking reaction time varied from 1 to 30 min. The final PCMs were obtained after dried at 25°C.

Homogeneous chitosan membranes were prepared by coating 2.5 wt % chitosan solution on a glass plate. STPP/chitosan PCMs without PAN UF support membranes were prepared to investigate swelling behaviors.

Crosslinking ratio measurement

The crosslinking ratio is defined as follows:

$$\theta_R = \frac{M_2 - M_1}{M_1} \times 100\% \quad (17)$$

where M_1 and M_2 are the weight of membranes before and after surface-crosslinking (g), respectively.

Membrane characterization

FTIR analysis

FTIR spectra of membranes were measured by a Nicolet, 5DX instrument equipped with both horizontal attenuated total reflectance (HATR) accessories (Thermo Electron Corp., Nicolet 5700, USA) operating in the wavenumber range 4000–400 cm^{-1} . The experiments were run with air as the background. Thirty-two scans were accumulated with a resolution of 4 cm^{-1} for each spectrum.

Morphology observation

The morphologies of membranes were examined by SEM (JEOL Model JSM-6360 LV, Japan). All samples were coated with gold under vacuum before testing.

EDX analysis

The EDX (Edax Falcon, USA) was applied to detect the element distribution profile on the external surface of membranes.

XRD analysis

The XRD patterns of membranes were recorded on a D/max-rB diffractometer (Rigaku, Japan) equipped with graphite monochromated Cu $K\alpha$ radiation ($\lambda = 0.15405$ nm) operated at 100 mA and 40 kV from 3 to 50°.

Swelling ratio measurement

The membrane was weighed (m_1) and immersed into ethyl acetate aqueous solution with different concentration at 313 K, during which the weight of mem-

brane was measured every hour to check out whether it had reached swelling equilibrium or not.¹⁴ After the membrane reached equilibrium, it was carefully taken out from the solution and quickly blotted between tissue papers to remove surface solvent, and then weighed the swollen membrane to obtain the weight (m_2). The swelling ratio (SR) was calculated by:

$$\text{SR} = \frac{m_2 - m_1}{m_1} \times 100\% \quad (18)$$

Pervaporation experiment

The schematic diagram of pervaporation apparatus has been described in detail elsewhere.¹⁵ The membrane with an effective area of 2.826×10^{-3} m^2 for pervaporation was installed in a membrane module. The permeate side was maintained at a vacuum pressure (2.4×10^3 Pa) by a vacuum pump. The permeate vapor sample was collected after being condensed in three traps with liquid nitrogen.

The separation performances of membranes were assessed in terms of permeation flux (J) and separation factor (α):

$$J = \frac{M}{S \times \Delta t} \quad (19)$$

where M is the total amount of permeate sample (g); S is the effective area of the membrane for pervaporation (m^2); and Δt is the experimental time interval (h).

$$a = \frac{w_i/w_j}{w_{i0}/w_{j0}} \quad (20)$$

where w_i , w_j , w_{i0} , and w_{j0} are the weight fractions of water and ethyl acetate in the permeate and retentate, respectively.

RESULTS AND DISCUSSION

Characterization of PCMs

FTIR of membranes

Figure 2 shows the FTIR spectrums of the top layer of chitosan homogeneous membrane, STPP squash, and the top layer of PCM made from PCM-2 with surface-crosslinking for 15 min. The major peaks for chitosan are observed around 3346 cm^{-1} which are assigned to the stretching vibration of $-\text{OH}$ groups. The peaks at 1649 and 1541 cm^{-1} are attributed to the secondary amide $\text{C}=\text{O}$ bond of the remaining acetamido groups and the $-\text{NH}$ bending vibration of $-\text{NH}_2$ groups, respectively.¹⁶ The peak at 1420 cm^{-1} can be assigned to $-\text{NH}$ deformation vibration in $-\text{NH}_2$, while the peak at 1070 cm^{-1} is due to the $-\text{CN}$ and $-\text{CO}$ stretching vibration. In STPP, the peak at 3413 cm^{-1} is the stretching vibration of $-\text{OH}$ groups, and the peaks at 1174 and 918 cm^{-1} are due to the $\text{P}-\text{O}$ and $\text{P}=\text{O}$ stretching and the $\text{P}-\text{O}$ bending.

After crosslinking, the spectrum of PCM-2 shows some changes. The peak of 3402 cm^{-1} becomes wider,

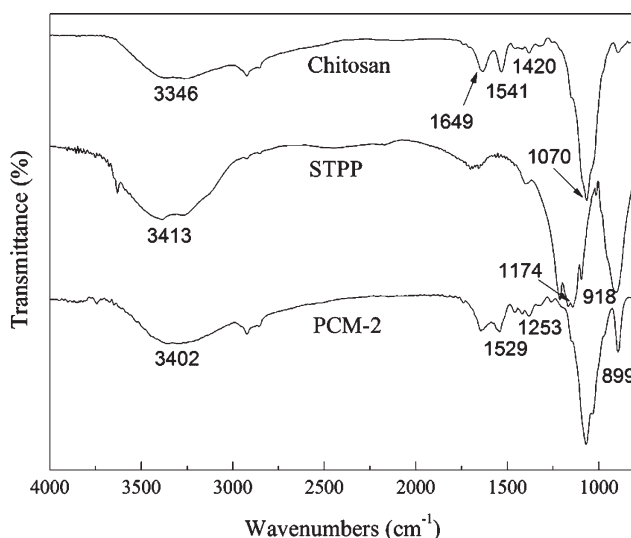
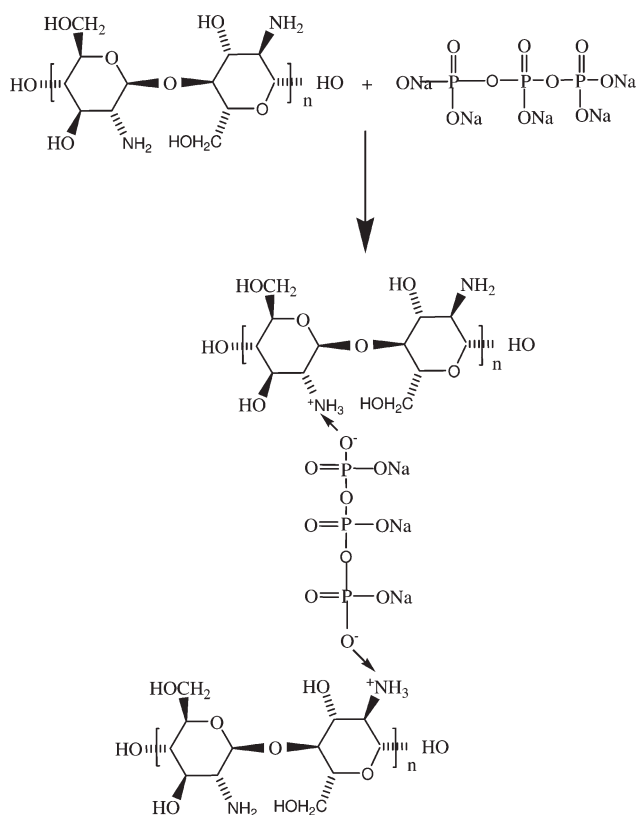


Figure 2 FTIR spectra of the top layer of chitosan homogeneous membrane, STPP squash, and the top layer of PCM made from PCM-2 with surface-crosslinking for 15 min.

indicating that hydrogen bonding is enhanced. The peak at 1529 cm^{-1} can be attributed to $-\text{NH}_3^+$. The peak is observed at 1253 cm^{-1} indicating the presence of $\text{P}=\text{O}$ stretching and the $\text{P}-\text{OH}$ groups found in the STPP molecule. All of the peaks related to N atoms are affected after the crosslinking process. The results illustrate that the crosslinking structure is formed between chitosan and STPP due to surface-crosslinking reaction, which is shown as follows¹⁷⁻¹⁹:



Morphologies of PCMs made from PCM-2 with different surface-crosslinking time

Figure 3 shows the morphologies of PCMs made from PCM-2 with different surface-crosslinking time. The outer surface of PCM-2 becomes smooth and dense gradually as surface-crosslinking time increases. However, some cracks appear when the surface-crosslinking time is more than 15 min. A possible explanation is that increasing surface-crosslinking time enhances the compactness degree and weakens pliability of chitosan. This result illustrates that crosslinking ratio increases as surface-crosslinking time increases and the surface-crosslinking time has an obvious effect on the morphologies of PCMs.

EDX of PCMs made from PCM-2 with different surface-crosslinking time

Table I shows element contents of PCMs made from PCM-2 with different surface-crosslinking time, which is obtained from the EDX results. Phosphorus and oxygen contents increase, while sodium content decreases as the surface-crosslinking time increases from 2 to 15 min. This illustrates that the surface-crosslinking reaction occurs, which is verified by FTIR in Figure 2. The increase rate of oxygen is less than that of phosphorus. A possible explanation is that STPP dissociates in water (original pH of STPP is about 9) to both OH^- and TPP ions. $\text{P}_3\text{O}_{10}^{5-}$, $\text{HP}_3\text{O}_{10}^{4-}$, and $\text{H}_2\text{P}_3\text{O}_{10}^{3-}$ coexist in the TPP solution. The OH^- and TPP ions competitively interact with the $-\text{NH}_3^+$ binding sites of chitosan by either deprotonation or ionic crosslinking. The element content changes slowly with long surface-crosslinking time due to fully neutralize. It is obvious that the surface-crosslinking time has an obvious effect on the structure of PCMs.

XRD of PCMs made from PCM-2 with different surface-crosslinking time

Figure 4 represents the XRD patterns of PAN support membrane, bulk neat chitosan membrane, bulk crosslinked STPP-chitosan membrane, and PCMs made from PCM-2 with different surface-crosslinking time. Bulk crosslinked membrane²⁰ and surface crosslinked membrane make different XRD results. Three intense diffraction peaks for PCM-2 without surface-crosslinking (PCM-2 (0min)) are clearly located at 17.56° , 22.64° , and 25.84° , respectively. With increment of surface-crosslinking time, these three peaks change or shift a little. For instance, three intense diffraction peaks for PCM-2 with surface-crosslinking for 6 min are located at 17.42° , 22.44° , and 25.72° , respectively. The crystal structure is changed due to the introduction of STPP disturbed the arrangement of chitosan chains. New polyionic bonds are formed, which is verified by FTIR in Figure 2.

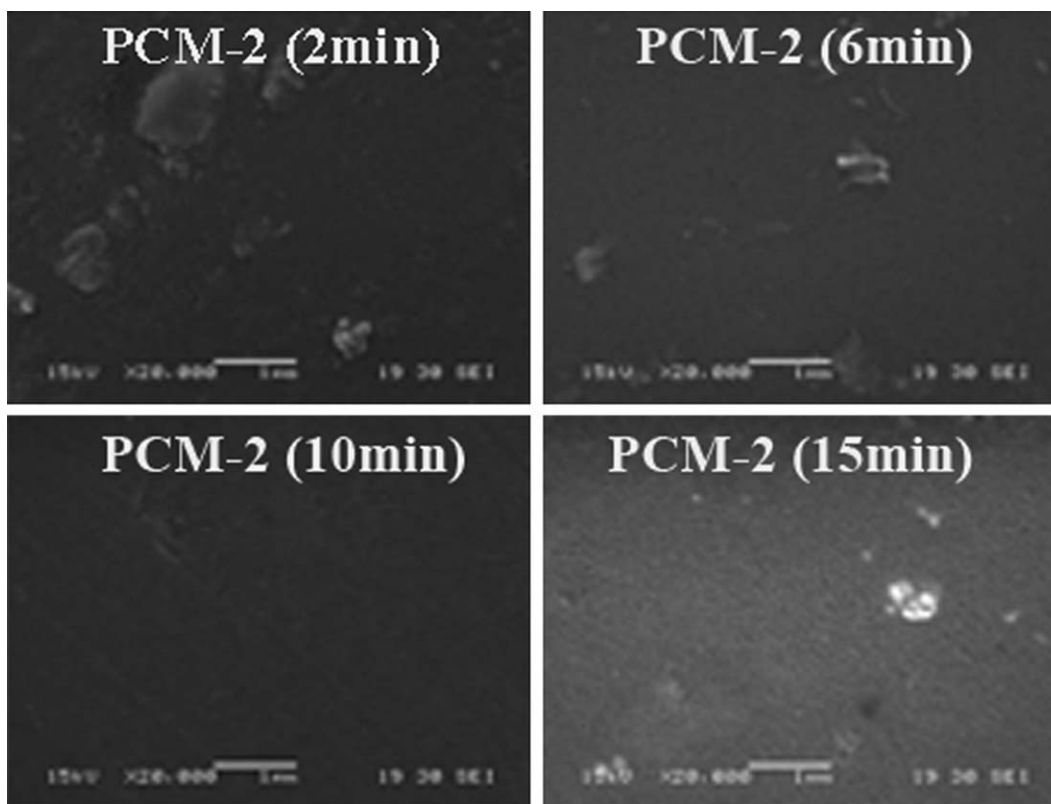


Figure 3 External surface morphologies of PCMs made from PCM-2 with different surface crosslinking time (magnification $\times 20,000$).

Swelling behaviors of STPP/chitosan PCMs

The swelling tests are performed to characterize crosslinking ratio, especially for the surface-crosslinking membranes with a low degree of crosslinking,^{21,22} since the crosslinking ratio is difficult to determine through routine analytical methods for crosslinking membranes. Figure 5 represents the effect of water concentration in the feed and STPP concentration on the swelling performance of STPP/chitosan PCMs in different ethyl acetate aqueous solutions at 313 K. The surface-crosslinking time of STPP/chitosan PCM is 15 min. The swelling ratio increases as water concentration increases, while decreases as STPP concentration increases.

Swelling ratio is corresponding to the ability of membrane adsorbing water.⁷ During surface-cross-

linking process, the short chain STPP molecule embeds in the long chain chitosan molecule to form new polyionic crosslinked spatial structure. The new polyionic bond is helpful to increase antiwater swelling property.²³ Moreover, the ion group in the polyelectrolyte complex mainly exists as ion pair, and the molecular skeleton of the main chain has a

TABLE I
Element Contents for the External Surface of PCMs Made from PCM-2 with Different Surface-Crosslinking Time

Surface-crosslinking time (min)	C (wt %)	O (wt %)	Na (wt %)	P (wt %)
2	19.92	54.45	12.17	13.46
6	20.39	55.09	8.81	15.71
10	20.61	55.44	8.01	15.94
15	20.76	55.72	7.21	16.31

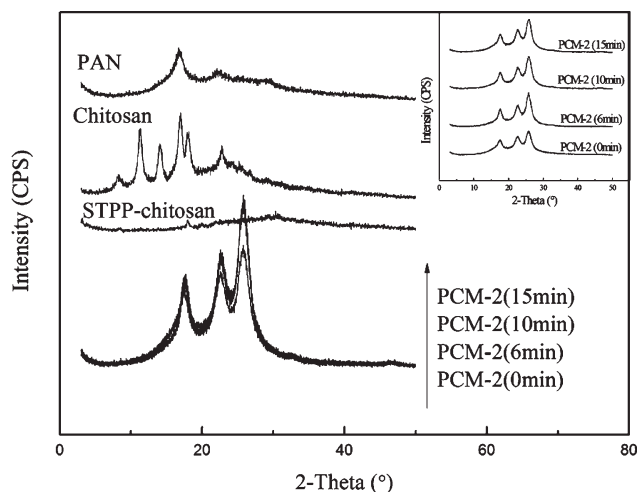


Figure 4 XRD of PAN support membrane, bulk neat chitosan membrane, bulk crosslinked STPPchitosan membrane, and PCMs made from PCM-2 with different surface-crosslinking time.

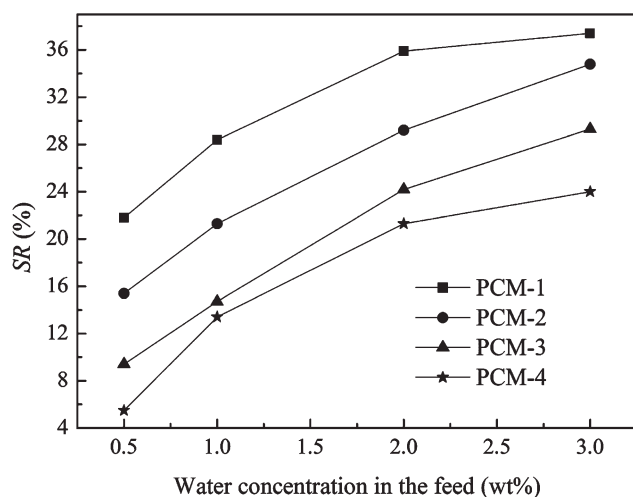


Figure 5 Effect of water concentration in the feed on the swelling behavior of STPP/chitosan PCMs in different ethyl acetate aqueous solutions at 313 K (surface-crosslinking time of 15 min).

shielding role on the ion pair, which hinders the solvation between ion pair and water molecule.

Model analysis of PCMs

Figure 6 represents the effect of surface-crosslinking time and crosslinking agent concentration on the crosslinking ratio between STPP and chitosan at room temperature, and simulated by eq. (16). The crosslinking ratio increases rapidly as surface-crosslinking time increases, then reaches a dynamic equilibrium after 15 min. This result illustrates that surface-crosslinking of 15 min in literatures^{8,9} is feasible. Increasing in crosslinking ratio is because the surface-crosslinking reaction is fully as surface-crosslinking increases. The dynamic equilibrium of crosslinking ratio is attributed to fully neutralize. It is found that some simulated values deviated from experimental values. Possible explanations are that (1) the adsorption deviates Langmuir equation, (2) the difference occurs due to hypothesis pseudo-steady state during the deduction process, and (3) the membrane has microvoids resulting in cohesion.

Figure 6 also shows that the crosslinking ratio increases as STPP concentration increases at the same surface-crosslinking time, since the active groups increase by addition STPP, which accelerate the surface-crosslinking reaction rate. These results indicate that the crosslinking ratio is determined by the crosslinking agent concentration and surface-crosslinking time. And the effect of crosslinking agent concentration on crosslinking ratio is inversely proportional to surface-crosslinking time. If crosslinking agent concentration is known, surface-crosslinking time can be fixed by this model to achieve a specified crosslinking ratio, and *vice versa*.

Table II shows the coefficients of the kinetic model at room temperature. Values of M and N increase as

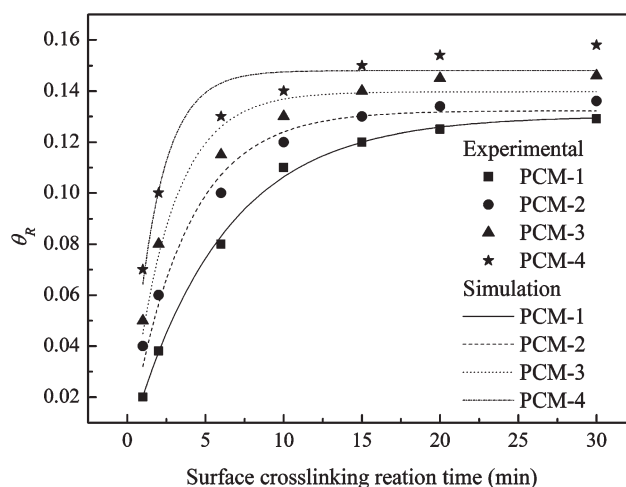


Figure 6 Effect of surface-crosslinking time and STPP concentration on the crosslinking ratio between STPP and chitosan at room temperature.

STPP concentration increase. The crosslinking ratios of PCMs are calculated when surface-crosslinking reacts 15 min.

Figure 7 shows the effect of crosslinking ratio on the swelling behavior of STPP/chitosan PCMs in different ethyl acetate aqueous solutions at 313 K (surface-crosslinking time of 15 min). It is obvious that the swelling ratio decreases as crosslinking ratio increases (Figure 5). This indicates that the swelling ratio of PCMs can be effectively controlled by crosslinking ratio and the model is reliable and accurate.

Figures 8 and 9 show the effect of crosslinking ratio on the separation performance of PCMs in different ethyl acetate aqueous solutions at 313 K (surface-crosslinking time of 15 min). As the flux decreases, the selectivity of water to ethyl acetate increases with the increment of crosslinking ratio. Crosslinking density of PCMs increases as crosslinking ratio increases, thus the membrane has less solubility of a liquid and less polymeric chain mobility leading to less free volume in the membrane. Both solubility and diffusivity of permeating liquid through the membrane decline in pervaporation process to depress the flux.²⁴ The reduction of free volume restrains the sorption and diffusion of ethyl acetate

TABLE II
Coefficients of Surface-Crosslinking Reaction Kinetic Model Between STPP and Chitosan at Room Temperature

Item	PCM-1	PCM-2	PCM-3	PCM-4
M	0.1302	0.1322	0.1397	0.1480
N	0.1695	0.2769	0.3874	0.5699
R -square	0.9975	0.9778	0.9509	0.9240
θ_R (surface-crosslinked 15 min)	0.1199	0.1301	0.1393	0.1480

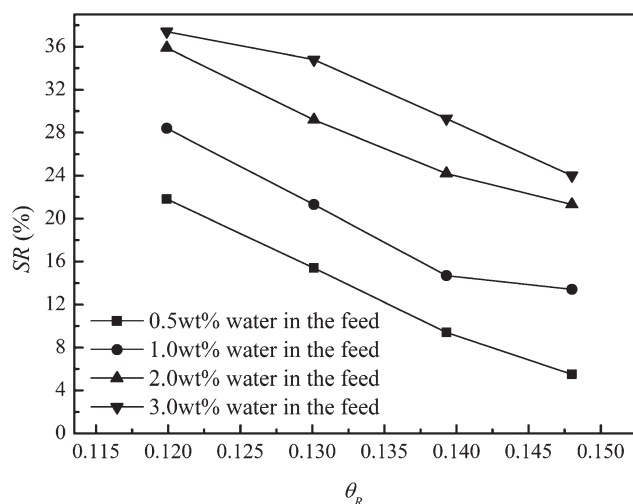


Figure 7 Effect of crosslinking ratio on the swelling behavior of STPP/chitosan PCMs in different ethyl acetate aqueous solutions at 313 K (surface-crosslinking time of 15 min).

into membrane due to its big size, resulting in increasing in separation factor.

Figures 10 and 11 show the effect of crosslinking ratio on separation performance of PCMs in 98 wt % ethyl acetate aqueous solution at different feed temperatures (surface-crosslinking time of 15 min). The flux decreases, whereas the separation factor increases as crosslinking ratio increases at the same feed solution temperature. Increase of crosslinking ratio enhances the compactness of membrane top layer and weakens the pliability of chitosan at the same time.²⁵

Separation performance of PCMs

Effect of water concentration in the feed and STPP concentration

Figures 8 and 9 also show the effect of water concentration in the feed on the separation performance of

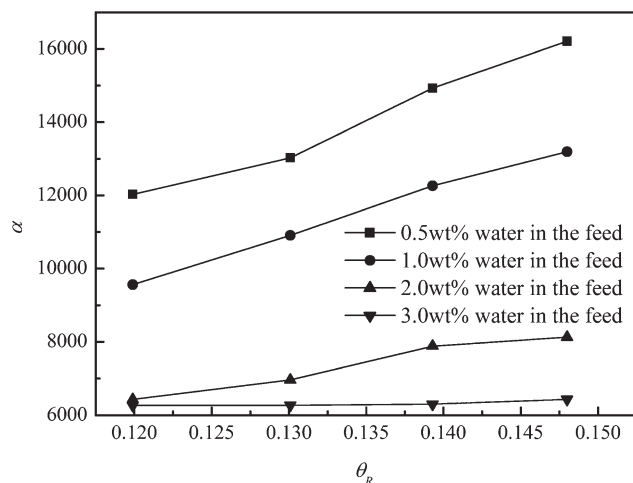


Figure 8 Effect of crosslinking ratio on the separation factor of PCMs in different ethyl acetate aqueous solutions at 313 K (surface-crosslinking time of 15 min).

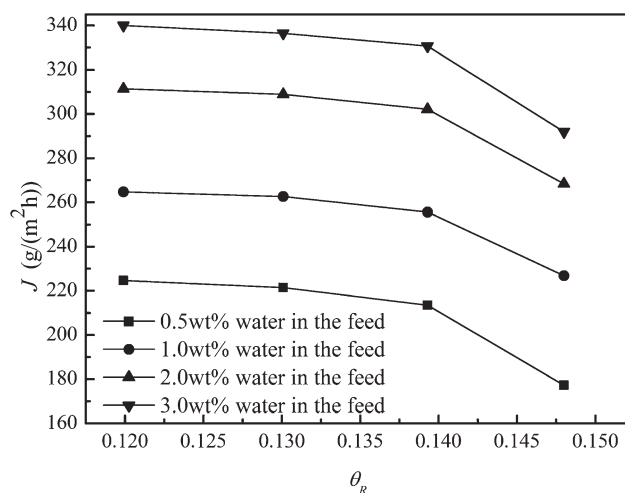


Figure 9 Effect of crosslinking ratio on the flux of PCMs in different ethyl acetate aqueous solutions at 313 K (surface-crosslinking time of 15 min).

PCMs in different ethyl acetate aqueous solutions at 313 K. The surface-crosslinking time is 15 min. The water concentration ranges from 0.5 to 3 wt % in feed solution.²⁶ The flux increases, while the separation factor decreases gradually as water concentration increases in the feed. The hydrophilic organic components have a stronger affinity for PCMs, water molecules are preferentially adsorbed and diffuse through the membrane while ethyl acetate is repelled. The coefficient of water activity in the feed solution decreases as water concentration increases, which results in increasing water sorption in the membrane. The membrane becomes much swollen and plasticized by water. The hydrophilicity of the swollen membrane decreases.^{27,28} The mobility of polymer chains and the free volume of polymer increase. Ethyl acetate molecules can permeate easily through the swollen areas in the membrane. Thereupon, the permeation flux increases, while the separation factors decrease as water content increased in the feed.

Effect of feed temperature and STPP concentration

Figures 10 and 11 also express the effect of feed temperature on the separation performance of PCMs in 98 wt % ethyl acetate aqueous solution at different feed temperatures. The surface-crosslinking time is 15 min. The flux increases, whereas the separation factor decreases with increasing feed temperature from 303 to 333 K. The frequency and amplitude of the polymer chain vibration increase as temperatures increase, resulting in increasing mobility of the top layer of PCMs and swelling degree.^{25,29} Thus the free volume of the membrane is expanded after swelling. The generated extra free volume is very helpful to increase the sorption and diffusion rate of

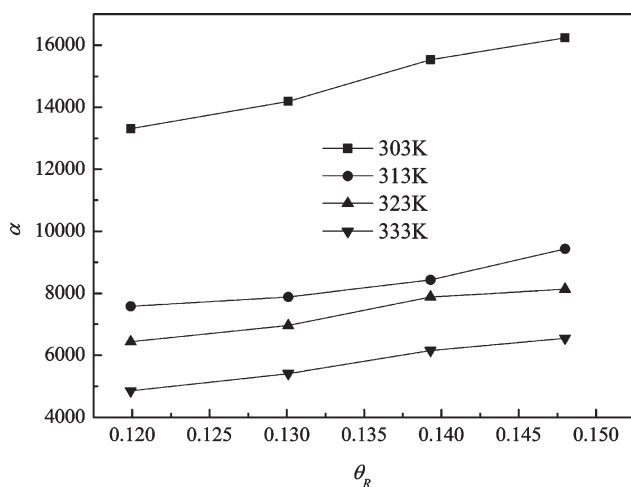


Figure 10 Effect of crosslinking ratio on the separation factor of PCMs in 98 wt % ethyl acetate aqueous solution at different feed temperatures (surface-crosslinking time of 15 min).

the permeate molecules. In addition, the vapor pressure of all components in the feed solution increases as feed temperatures increase, while the vapor pressure at the permeate side is not affected. Thereupon the driving force increases with increasing feed temperatures.²⁹ However, increasing free volume in the polymer matrix leads to an easy transport of organic component.²⁵

The relationship between the permeation fluxes and the feed solution temperatures has a good agreement with Arrhenius equation:

$$J = J_0 \exp\left(-\frac{\Delta E_a}{RT}\right) \quad (21)$$

where R is gas constant (J/(mol K)); T is absolutely temperature (K); ΔE_a is permeation activation energy (kJ/mol); and J_0 is preexponential factor.

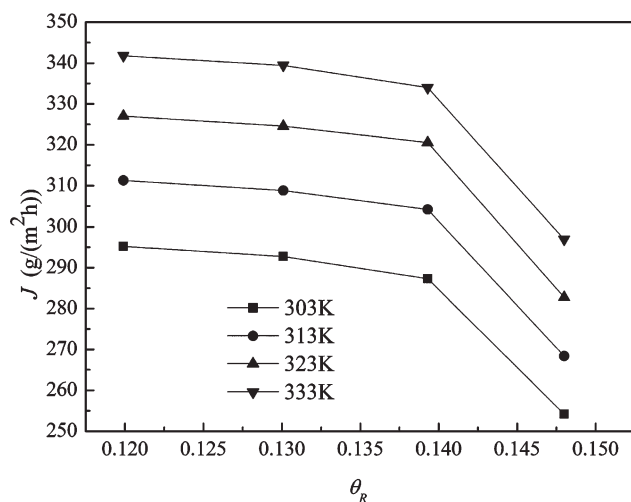


Figure 11 Effect of crosslinking ratio on the flux of PCMs in 98 wt % ethyl acetate aqueous solution at different feed temperatures (surface-crosslinking time of 15 min).

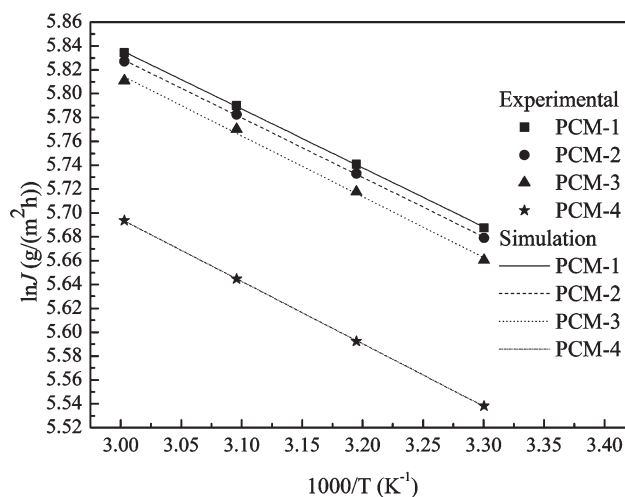


Figure 12 Plot of $\ln J$ vs. $1000/T$ for PCMs in 98 wt % ethyl acetate aqueous solution at different feed temperatures (surface-crosslinking time of 15 min).

Figure 12 shows a plot of $\ln J$ versus $1000/T$ for PCMs. The permeation activation energy (ΔE_a) of PCM-1, PCM-2, PCM-3, and PCM-4 is 4.11, 4.14, 4.24, and 4.35 kJ/mol, respectively. These results can be explained by assuming that increasing STPP concentration leads the permeation activation energy to increase. The larger permeation activation energy implies that the permeation flux is much sensitive to temperature increment.³⁰ These suggest that proper increment of feed temperature is helpful to dehydration of the ethyl acetate–water mixtures.

CONCLUSION

Surface-crosslinking time had an obvious effect on the performance of PCMs. The membrane possessed the excellent performance when surface crosslinked for 15 min. Surface-crosslinking time and crosslinking agent concentration affected the crosslinking ratio. Based on the kinetic model, it was found that the crosslinking ratio of PCM exponentially increased as time increased, while linearly increased as concentration and diffusion coefficient of crosslinking agent increased. The effect of crosslinking agent concentration on crosslinking ratio was inversely proportional to surface-crosslinking time. The experimental results matched well with the kinetic model when STPP concentration was lower than 5 wt %. It was obvious the crosslinking ratio could be controlled to prepare PCMs with good performance. PCM surface crosslinked for 15 min by 5 wt % STPP had flux of 336 g/(m² h) and separation factor of 6270 in 97 wt % ethyl acetate aqueous solution at 313 K. This kinetic model could also be used to describe the kinetics of membrane modification methods such as polymerization, block, and graft. We suggest that the separation performance of PCM

with different crosslinking ratios should be further investigated. Our results could be useful to researchers attempting to optimize membrane preparation and minimize the number of experiments.

References

1. Kim, S. G.; Lim, G. T.; Jegal, J.; Lee, K. H. *J Membr Sci* 2000, 174, 1.
2. Hu, C.; Guo, R.; Li, B.; Ma, X.; Wu, H.; Jiang, Z. *J Membr Sci* 2007, 293, 142.
3. Hu, C.; Li, B.; Guo, R.; Wu, H.; Jiang, Z. *Sep Purif Technol* 2007, 55, 327.
4. Lukás, J.; Richau, K.; Schwarz, H. H.; Paul, D. *J Membr Sci* 1997, 131, 39.
5. Zhao, Q.; Qian, J.; An, Q.; Gui, Z.; Jin, H.; Yin, M. *J Membr Sci* 2009, 329, 175.
6. Ostrowska-Czubenko, J.; Gierszewska-Druzynska, M. *Carbohydr Polym* 2009, 77, 590.
7. Liu, Y. L.; Su, Y. H.; Lai, J. Y. *Polymer* 2004, 45, 6831.
8. Kusumocahyo, S. P.; Kanamori, T.; Iwatsubo, T.; Sumaru, K.; Shinbo, T. *J Membr Sci* 2002, 208, 223.
9. Zhao, Q.; Qian, J. W.; An, Q. F.; Yang, Q.; Zhang, P. *J Membr Sci* 2008, 320, 8.
10. Richau, K.; Schwarz, H. H.; Apostel, R.; Paul, D. *J Membr Sci* 1996, 113, 31.
11. Schwarz, H. H.; Lukás, J.; Richau, K. *J Membr Sci* 2003, 218, 1.
12. Moon, G. Y.; Pal, R.; Huang, R. Y. M. *J Membr Sci* 1999, 156, 17.
13. Schwarz, H. H.; Apostel, R.; Paul, D. *J Membr Sci* 2001, 194, 91.
14. Zhao, Q.; Qian, J.; An, Q.; Gao, C.; Gui, Z.; Jin, H. *J Membr Sci* 2009, 333, 68.
15. Won, W.; Feng, X.; Lawless, D. *Sep Purif Technol* 2003, 31, 129.
16. Lee, Y. M.; Nam, S. Y.; Woo, D. J. *J Membr Sci* 1997, 133, 103.
17. de Moura, M. R.; Aouada, F. A.; Avena-Bustillos, R. J.; McHugh, T. H.; Krochta, J. M.; Mattoso, L. H. C. *J Food Eng* 2009, 92, 448.
18. Musale, D. A.; Kumar, A. *Sep Purif Technol* 2000, 21, 27.
19. Hsieh, F. M.; Huang, C.; Lin, T. F.; Chen, Y. M.; Lin, J. C. *Process Biochem* 2008, 43, 83.
20. Chen, J. H.; Liu, Q. L.; Zhang, X. H.; Zhang, Q. G. *J Membr Sci* 2007, 292, 125.
21. Xiao, S.; Feng, X.; Huang, R. Y. M. *J Membr Sci* 2007, 306, 36.
22. Xiao, S.; Huang, R. Y. M.; Feng, X. *J Membr Sci* 2006, 286, 245.
23. Huang, R. Y. M.; Moon, G. Y.; Pal, R. *J Membr Sci* 2000, 176, 223.
24. Yeom, C. K.; Lee, K. H. *J Membr Sci* 1996, 109, 257.
25. Yuan, H. K.; Xu, Z. L.; Shi, J. H.; Ma, X. H. *J Appl Polym Sci* 2008, 109, 4025.
26. Salt, Y.; Hasanoglu, A.; Salt, I.; Keleser, S.; Özkan, S.; Dinçer, S. *Vacuum* 2005, 79, 215.
27. Lamer, T.; Rohart, M. S.; Voilley, A.; Baussart, H. *J Membr Sci* 1994, 90, 251.
28. Tian, X.; Zhu, B.; Xu, Y. *J Membr Sci* 2005, 248, 109.
29. Zhang, X. H.; Liu, Q. L.; Xiong, Y.; Zhu, A. M.; Chen, Y.; Zhang, Q. G. *J Membr Sci* 2009, 327, 274.
30. Bai, Y.; Qian, J.; Zhang, C.; Zhang, L.; An, Q.; Chen, H. *J Membr Sci* 2008, 325, 932.